

## International Seminar on UTP-UIR Matching Grant Progress Report 2019

Home → [Keynote](#)

### IMPORTANT SUBMISSION DATES

Call for Papers:

01 Apr 2019

Submission of Full Paper Final  
Deadline:

### Keynote Speech 1



Prof. Dr. Mustafa Bin Mat Deris,

#### Abstract – Data Reduction for Information Systems: Issues, Challenges and Future Direction

With the massive data generated daily into computer systems, it is difficult to manage and analyses such massive data size. It is not only causing by the data heterogeneity but also the diverse of dimensionalities in the datasets. For example, social data aggregators, scientific experimental systems, the profiles of internet users, etc., are sparse with high dimensionalities. Thus, it is imperative to reduce the data while retaining the most important and useful data. Data reduction is a process to reduce the volume/size of data to make effective data analysis. It is mainly based on the dimension reduction to reduce the number of features in a dataset without having to lose much information. Dimension reduction techniques are useful to handle the heterogeneity and massiveness of data by reducing variables into manageable size. To some fields, such as data mining, bio-informatics, and machine learning, data sets have huge number of dimensions/attributes that often be encountered. Some attributes are irrelevant or redundant that can complicate the problem and subsequently, degrade the performance and solution accuracy. Thus, some redundant or irrelevant attributes need to be removed which is the main objective of attribute selection. A wide range of dimension reduction approaches are based on classical approaches such as PCA and Bayer's, and machine learning approaches such as clustering, and feature selection techniques. Rough set theory proposed by Pawlak was successful in the study of soft computing characterized by uncertainty of information, especially in rule extraction, uncertainty reasoning, granular computing, data clustering and data classification. It has been proven to be an efficient mathematical tool as compared with PCA, neural networks and support vector machine methods. Unlike those methods, rough set theory allows knowledge discovering process to be conducted automatically by the data themselves without any dependence on the prior knowledge. The rough set theory however, only be used to solve complete information systems where all available objects in information system have attribute values. It is basically based on the indiscernibility relation that conforms with the reflexive, symmetric and transitive properties. A problem arises when certain attribute values in information systems are missing that cause imprecise answer to some queries, which sometimes happens in the real world. This information system is called incomplete information system (IIS). Because some attribute values are missing in incomplete information systems, such relational properties are difficult to generate, and it is hard to process the incomplete information systems with the indiscernibility relation. There have been many efforts in studying incomplete information systems. Some approaches on attribute selection for IIS have been proposed: tolerance relation approach, and tolerance relation using conditional entropy approach. However, tolerance relation approach leads to poor results in terms of approximation. Therefore, it is important to propose a new approach in order to improve the approximation in the near future.

#### Speaker Biography:

**Prof. Dr. Mustafa Mat Deris** received PhD from University Putra Malaysia in 2002. He is a professor of computer science in the Faculty of Computer Science and Information Technology, UTHM, Malaysia. He has successfully supervised Seventeen PhD students and published more than 270 papers in journals and conference proceedings. He has appointed as editorial board member for Journal of Next Generation Information Technology, JNIT, Korea, International Journal of Rough Sets and Data Analysis, IGI Global, USA and Encyclopedia on Mobile Computing and Commerce, Idea Group, USA.

He was appointed as a keynote speaker from several conferences and served as a program committee member and co-organizer for numerous international conferences/workshops including Grid and Peer-to-Peer Computing, (GP2P 2005, 2006), Autonomic Distributed Data and Storage Systems Management (ADSM 2005, 2006, 2007), and Grid Pervasive Computing Security, organizer for workshops on Rough and Soft Sets Theories and Applications (RSAA 2010, Fukuoka, Japan), Soft Computing and Data Engineering (SCDE) (2010, 2011, Korea), (2012, Brazil), and for International Conference for Soft Computing and Data Mining (SCDM14, SCDM16 and SCDM18).

He is the recipient of "ICT Excellent Teacher" award in 2006, from Malaysian National Computing Confederation (MNCC). His research interests include distributed databases, rough set theory, soft set theory, and data mining.

Scopus 219 publications, H index =18 from 1304 citations

<http://www.scopus.com/authid/detail.url?authorid=6507331989>

## Keynote Speech 2



**Dr. David Chong**

**Principal Engineer, TechSource Systems Sdn. Bhd., Malaysia**

#### Abstract - Digital Twins with MATLAB & Simulink

Digital twin technology has moved beyond manufacturing and into the merging worlds of the Internet of Things, artificial intelligence and data analytics. Creating and using digital twins increases intelligence as part of the operational system. Having an up-to-date representation of real operating assets lets us control or optimize the assets and the wider system. The representation not only captures the current state, but often the operating history of the asset. Digital twins enable us to optimize, improve efficiencies, automate, and evaluate future performance.

With MATLAB, we can define a model using data from our connected asset. We can also use Simulink to create a physics-based model using multi-domain modeling tools. Both data-driven and physics-based models with MATLAB & Simulink can be tuned with data from the operating asset to act as a digital twin for prediction, anomaly detection, fault isolation, and more.

**Speaker Biography:** Dr. David Chong Jin Hui is Senior Account Manager for business development at TechSource Systems. He is formerly ASEAN Technical Team Leader & principal application engineer at TechSource Systems. He is specialized in machine learning, deep learning, signal processing, communication and application deployment with MATLAB. Prior joining TechSource Systems, he worked at MIMOS as technical leader, staff researcher & developer, Tunku Abdul Rahman University College as senior lecturer & Intel as senior component engineer. Dr. David Chong holds BEng of Computer & Communication System Engineering and PhD in wireless communication in University Putra Malaysia.

# Organizing Committee

<b>General Chair</b>	Fawnizu Azmadi Hussin (IEEE MY)
<b>General Co-Chair</b>	Alpha Agape Gopalai (IEEE MY)
<b>Conference Chair</b>	Irraivan Elamvazuthi (IEEE RAS)
<b>Finance</b>	Chong Yu Zheng (IEEE MY) Niharika Singh (IEEE UTP SB)
<b>Secretary</b>	Azrina Bt A Aziz (IEEE WIE) Saranya Krishnamurthy (IEEE UTP SB) Arun Mozhi Devan (IEEE UTP SB)
<b>Event Management</b>	Nursyarizal Mohd Nor (IEEE PES) Muhammad Wasif Umar (IEEE UTP SB) Nirbhay Mathur (IEEE UTP SB)
<b>Technical Program</b>	Md Pauzi Abdullah (IEEE MY) Rosdiazli Ibrahim (IEEE MY) Moslem Uddin (IEEE UTP SB) Maged S.AL-Quraishi (IEEE UTP SB) Nivesh Gadipudi (UTP IEEE SB)

---

**Publication**

Syed Saad Azhar Ali (IEEE RAS)  
Kishore Bingi (IEEE UTP SB)  
Lakshmi Manasa Vedantham (IEEE UTP SB)

**Publicity**

Nasreen Bt Badruddin (IEEE WIE)  
Upasana Lakhina (IEEE UTP SB)  
Sumit Aole (IEEE UTP SB)

**Sponsorship**

M Faris B Abdullah (IEEE PES)  
Anika Mansura (IEEE UTP SB)

**Logistics**

Furqan Zahoor (PGSC)  
Zeeshan Memon (PGSC)  
Ejaz Muhammad Mudassir (PGSC)

**Secretariat**

Rohayu Bt Roslan (UTP)  
Insyirah Hamid (UTP)  
Nurnajla Adnan (PGSC)  
Nor Shamsimah Ab Rahman (PGSC)

---

---

Search within results

Items Per Page

Export

Email Selected Results

Showing 1-25 of 88

Refine

Author

Affiliation

Quick Links

Search for Upcoming Conferences

IEEE Publication Recommender

IEEE Author Center

Proceedings

The proceedings of this conference will be available for purchase through Cumint Associates.

Research and Development (SCD&D), 2019 IEEE Student Conference on

Print on Demand Purchase at Partner

External Hard-drive Purchase at Partner

Select All on Page

Sort By Sequence

Rotor Angle Transient Stability Methodologies of Power Systems: A Comparison

Alyu Sabio, Noor Izmi Abdul Wahab  
Publication Year: 2019, Page(s): 1 - 6  
Cited by: Papers (8)

Abstract H I M L

Design and Fabrication of Outboard Braking System for All Terrain Vehicle

Sunny Pragasai, Abhishek Kumar  
Publication Year: 2019, Page(s): 7 - 10  
Cited by: Papers (1)

Abstract H I M L

Predictive Maintenance of Air Booster Compressor (ABC) Motor Failure using Artificial Neural Network trained by Particle Swarm Optimization

Nurfitriah Syahwah Hashi, Nurul Haniwa'ain Burhani, Haseebul Ibrahim  
Publication Year: 2019, Page(s): 11 - 16  
Cited by: Papers (1)

Abstract H I M L

Perazuhan: A Mobile Application for Solid Waste Micro-Management Framework

Fadel Mhaz Ballam, Christen SE A. Corpuz, Lance Antonio R. Pines, Bernie S. Pabito, Elizabeth H. Hovers  
Publication Year: 2019, Page(s): 17 - 20  
Cited by: Papers (1)

Abstract H I M L

Research Direction Based Green Communications for Next Era: A Bibliometric Analysis

Fadhil Mubli, Khokoud Mawwad, Kamarul Arifin bin Noordin, Nadier aka Elashien  
Publication Year: 2019, Page(s): 21 - 26  
Cited by: Papers (1)

Abstract H I M L

Comparison Between Segmental and Salient Rotors of Single-phase Field Excitation Flux Switching Motor with Non-Overlap Windings for Lightweight Applications

Mohd Fairuz Omar, Erwan Sulaiman, Md. Zaref Ahmed, Syed Muhammad Naufal Syed Otman, Hassan Ali Soomro, Laili Ismail Joseph  
Publication Year: 2019, Page(s): 27 - 32  
Cited by: Papers (1)

Abstract H I M L

Ovarian Cancer Classification Accuracy Analysis Using 16-Neuron Artificial Neural Networks Model

Mt. Akbar Rahman, Navee Chandren Maniyandi, Kh. Ishaidul Ismail, Md. Mokheer Rahman  
Publication Year: 2019, Page(s): 33 - 38  
Cited by: Papers (7)

Abstract H I M L

Comparison of Fast and Slow Wave Correlation with Various Porosities between Two Measurement Technique

Muhammad Amin Abd Wahab, Nabila Sudirman, Mohd Ashraf Abdul Razak, Fauzan Khairi Che Harun, Nurul Aashikin Abdul Kadir  
Publication Year: 2019, Page(s): 39 - 44  
Cited by: Papers (2)

Abstract H I M L

An Efficient Energy Consumption Technique in Integrated WSN-IoT Environment Operations

Ganesekar Thangarajoo, P. D. D. Dominic, Mahomed bin Otman, Najalingam Sokkolalingam, Kayathirvi Subramanian  
Publication Year: 2019, Page(s): 45 - 48  
Cited by: Papers (8)

Abstract H I M L

ALGEBright: Design of an Avatar Customization Game-Based Learning for Algebra

João Henri Christian C. de Castro, Rodney Janival Z. Chirco, Wiltony James Cambic, Bradford Thomas Lutz, Bernie S. Pabito, Marissa N. Jaente  
Publication Year: 2019, Page(s): 49 - 52  
Cited by: Papers (2)

Abstract H I M L

Nursery Solenox: A Mobile Application for Learning Solenox for Pre-Bohoolers

Clifford A. Calleja, Paul John E. Carabatero, Dawn Neil R. Capa, Ma. Katrina A. Luzarte, Bernie S. Pabito  
Publication Year: 2019, Page(s): 53 - 57  
Cited by: Papers (1)

Abstract H I M L

A Review on Synchrophasor Technology for Power System Monitoring

Muhammad Nasser bin Mohd Nasir, Alyu Sabio, Noor Izmi Abdul Wahab  
Publication Year: 2019, Page(s): 58 - 62  
Cited by: Papers (3)

Abstract H I M L

Downtime Cost Analysis of Offloading Operations Considering Vessel Motions and Mooring Responses in Malaysian Waters

M. S. Patel, M. S. Liew, Zaharizka Mustaffa, A. M. Al-Yacoubi, Abdumawhood Saad Abdumawhood, Andrew Whyte

Need Full-Text access to IEEE Xplore for your organization? CONTACT IEEE TO SUBSCRIBE >

10 YEARS  
IEEE Access is celebrating its 10 Year Publishing Anniversary!  
View the top 10 articles published over the last decade based on downloads, citations, and overall impact in IEEE fields of interest.  
View Articles

Search within results

Showing 25-50 of 85

- Refine  Select All on Page Sort By
- Author**  **Linear Matrix Inequality Based Controller used in Multivariable Systems** 🔒

M. Nugrajeningsih, S. Kardinata, I. Anthea, P. Arun Mochi Dewan  
 (Publication Year: 2019, (Page(s): 134 - 139)  
 Cited by: (Papers (2))

▼ Abstract [HTML](#) [PDF](#) [CC](#)
  - Investigation of Segmented Rotor FEF 88M with Non-Overlap Windings in Various Slot-Pole Configurations** 🔒

Mohd Fairoz Omar, Erwan Sulaiman, Md Zairul Akmal, Fahad Khan  
 (Publication Year: 2019, (Page(s): 140 - 145)  
 Cited by: (Papers (2))

▼ Abstract [HTML](#) [PDF](#) [CC](#)
  - Building Ambient Temperature Measurement using Industrial Wireless Mesh Technology** 🔒

Isen Duc Chang, Hossain U Ibrahim  
 (Publication Year: 2019, (Page(s): 146 - 151)  
 Cited by: (Papers (1))

▼ Abstract [HTML](#) [PDF](#) [CC](#)
  - Robot Character Recognition For Optical And Natural Images Using Deep Learning** 🔒

Ri Immanuel Rasool Abidin, Riana Fariha Ghani  
 (Publication Year: 2019, (Page(s): 152 - 156)  
 Cited by: (Papers (3))

▼ Abstract [HTML](#) [PDF](#) [CC](#)
  - A Preliminary Study of Microwave Metamaterial Absorber Base on Cross-shaped for Stealth Technology** 🔒

Hadi Nuguh Yudhan, Yoh Karsenda  
 (Publication Year: 2019, (Page(s): 157 - 160)  
 Cited by: (Papers (2))

▼ Abstract [HTML](#) [PDF](#) [CC](#)
  - IoT Based Vehicle Emission Monitoring and Alerting System** 🔒

P. Arun Mochi Dewan, Fatinu Azzah Hussain, Hossain U Ibrahim, Kishore Singh, M. Nugrajeningsih  
 (Publication Year: 2019, (Page(s): 161 - 165)  
 Cited by: (Papers (11))

▼ Abstract [HTML](#) [PDF](#) [CC](#)
  - Collision-Slots Skipping Based Binary Tree Anti-Collision Algorithm for RFID** 🔒

Rubithah Anwar, Nurazila A. Jali, Saad Nurgawati, Luchakom Wuttalakkul  
 (Publication Year: 2019, (Page(s): 166 - 169)

▼ Abstract [HTML](#) [PDF](#) [CC](#)
  - A modified crow search algorithm with niching technique for numerical optimization** 🔒

Jahedul Islam, Faridhan M. Vasant, Saethan Manoj Nagesh, Juroo Wakiada  
 (Publication Year: 2019, (Page(s): 170 - 175)  
 Cited by: (Papers (4))

▼ Abstract [HTML](#) [PDF](#) [CC](#)
  - Understanding the differences in students' attitudes towards social media use: A case study from Oman** 🔒

Noor Al-Daway, Nafiseh Mohamed-Nasser, Moadifa Al-Emran, Muhammed A. Al-Sharifi  
 (Publication Year: 2019, (Page(s): 176 - 179)  
 Cited by: (Papers (19))

▼ Abstract [HTML](#) [PDF](#) [CC](#)
  - Optimal Modelling of Process Variations in Industry 4.0 Facility under Advanced P-Box Uncertainty** 🔒

Karim Shamsuddin, Ashwin Mohan, Frederick Dubucowski, Mark Verderyha  
 (Publication Year: 2019, (Page(s): 180 - 185)  
 Cited by: (Papers (6))

▼ Abstract [HTML](#) [PDF](#) [CC](#)

**Need Full-Text**  
 access to IEEE Xplore for your organization?  
 CONTACT IEEE TO SUBSCRIBE >

**10 YEARS**  
 IEEE Xplore is celebrating its 10 Year Publishing Anniversary!  
 View the top 10 articles published over the last decade based on downloads, citations, and overall impact in IEEE Xplore.  
[View Articles](#)

**Quick Links**

Search for Upcoming Conferences

IEEE Publication Recommender

IEEE Author Center

**Proceedings**

The proceedings of this conference will be available for purchase through Curran Associates.

Research and Development (SCOR&D), 2019 IEEE Student Conference on

Print on Demand Purchase at Partner

External Hard-Drive Purchase at Partner

- 
- Robust Real-Time Fire Detector Using CNN And LSTM**

Al Maamoun Haqad Abdul, Hama Farwad Ghani  
 Publication Year: 2019, (Page(s)) 204 - 207  
 Cited by: Papers (1)

[Abstract](#)
[HTML](#)

---

  - Firmly Fixed Route Selection With Cluster Approach To Diminish Overhead In VANET**

K. Anandhan, K. J. Keesarasa, K. P. Anandhan, C. Hama Devi  
 Publication Year: 2019, (Page(s)) 208 - 213  
 Cited by: Papers (3)

[Abstract](#)
[HTML](#)

---

  - Design Topology Optimization and Kinematic of a Multi-Modal Guedoopter and Quadruped**

Elango Natarajan, Cheah Tzu Ang, Yik Hong Lim, G. Kosalakrishnan, C.K. Ang, S. Parasuraman  
 Publication Year: 2019, (Page(s)) 214 - 218  
 Cited by: Papers (2)

[Abstract](#)
[HTML](#)

---

  - Review on Security in Bluetooth Low Energy Mesh Network in Correlation with Wireless Mesh Network Security**

Muhammad Husein Ghart, Ist-Chau Wan, Mohammed Anbar, Gian Chand Sothly, Amna Husein  
 Publication Year: 2019, (Page(s)) 219 - 224  
 Cited by: Papers (7)

[Abstract](#)
[HTML](#)

---

  - EEG Eye State Identification based on Statistical Feature and Common Spatial Pattern Filter**

Wang Chao Zhou, Nonahikin Yahya, Nauman Gadrubdin  
 Publication Year: 2019, (Page(s)) 225 - 230

[Abstract](#)
[HTML](#)

---

  - Classification of Neurological States from Biosensor Signals Based on Statistical Features**

Soung Chen Xim, Nonahikin Yahya, Lita Izmila Idris  
 Publication Year: 2019, (Page(s)) 231 - 236  
 Cited by: Papers (1)

[Abstract](#)
[HTML](#)

---

  - Design and Development of a Snake-Robot for Pipeline Inspection**

Arqam Sahasagar, Anshul Kumar, Devika Selvar, Mohd Azeem bin Haniffa  
 Publication Year: 2019, (Page(s)) 237 - 242  
 Cited by: Papers (8)

[Abstract](#)
[HTML](#)

---

  - Preliminary Implementation of the Next Generation Cannulation Simulator**

Abdulrahman Mahmoud, Usair Khurshid, Aman Abucaireh, Saib Mahmud, Omara Abdallah, Eshwath Mohamed, Abdulrah Alsalami, Fayal Samad, Abbas Amra, Ali Ali Hweidi, Gulshame Akhtar, Ibrahim Hassan  
 Publication Year: 2019, (Page(s)) 243 - 247  
 Cited by: Papers (1)

[Abstract](#)
[HTML](#)

---

  - Optimization of Metal Oxide Nanostructures via Two-Step Hydrothermal Synthesis**

Lucrard Sean Anthony, Veerachanan Perumal  
 Publication Year: 2019, (Page(s)) 248 - 252

[Abstract](#)
[HTML](#)

---

  - Wearable Thermoelectric Nanogenerator Based on Carbon Nanotube for Energy Harvesting**

Fariba Mami, Ahmed Z. Eidi, Nabila Fakhri  
 Publication Year: 2019, (Page(s)) 253 - 258  
 Cited by: Papers (8)

[Abstract](#)
[HTML](#)

---

  - Optical Sensing Technique Investigation for Preservative Latex Measurement**

Nina Karina Siti Mardiah, Yezir Liana Siti Abdulrah, Muhammad Hafid bin Harun, Faridatul Alma Siti beral  
 Publication Year: 2019, (Page(s)) 259 - 264

[Abstract](#)
[HTML](#)

---

  - Expeditious Fabrication & Characterization of Metal Interdigitated Transducer on Polyimide film for Biosensing Application**

Indra Ganesi Subramani, Jemal Afi bin Ahmad Fauzi, Veerachanan Perumal  
 Publication Year: 2019, (Page(s)) 265 - 269

[Abstract](#)
[HTML](#)

Showing 21-22 of 22

Refine

Select All on Page

Sort by

Sequence

Author

Affiliation

Quick Links

Search for Upcoming Conferences

IEEE Publication Recommender

IEEE Author Center

Proceedings

The proceedings of this conference will be available for purchase through Curran Associates.

Research and Development (SCQ/AD), 2019 IEEE Student Conference on

Print on Demand Purchase at Partner

External Host/Drive Purchase at Partner

Smith Predictor-based Controllers for Temperature Process with Time Delay

Juan Manuel Ramirez, Soheil Babaei, Mehdi

Publication Year: 2019, Page(s) 259 - 274

Cited by: Papers (2)

Abstract HTML

Multi-Input Power Converter for Renewable Energy Sources using Active Current Sharing Scheme

Fahim Nabil Moustafa, Hossain Khatun, Khalid Nisak Md. Hossain, Azura Ali

Publication Year: 2019, Page(s) 275 - 279

Abstract HTML

Low-power RRAM Device based 1T1R Array Design with CNTFET as Access Device

Furqan Zafar, Tom Zarek, Amir Zubair, Farooq Ahmed Khan, Aabid Arshad Fida

Publication Year: 2019, Page(s) 280 - 283

Cited by: Papers (5)

Abstract HTML

Utilization of Artificial Neural Networks to Improve the Accuracy of a Hybrid Power System Model

Muhammad Araf, M.F. Abdulkadir, Yener Khalid, M.F. Hameed

Publication Year: 2019, Page(s) 284 - 288

Cited by: Papers (1)

Abstract HTML

Effect Of Neurofeedback 2D and 3D Stimulus Content On Stress Mitigation

Yusef Habbas, Syed Saad Ahsan Ali, Syed Faraz, Muhammad Mansoor, Syed Hassan Ali

Publication Year: 2019, Page(s) 289 - 293

Cited by: Papers (2)

Abstract HTML

Autonomous Visual Navigation using Deep Reinforcement Learning: An Overview

Muhammad Mubassir Ejaz, Tong Boon Tang, Cheng-Kai Lu

Publication Year: 2019, Page(s) 294 - 298

Cited by: Papers (2)

Abstract HTML

Communication Latency in Multi-agent System for Microgrid

Nishaika Singh, I. Esmailzadeh, P. Nallagowden, G. Hameed, Ajay Jangra

Publication Year: 2019, Page(s) 300 - 305

Cited by: Papers (1)

Abstract HTML

Medical Image Classification: A Comparison of Deep Pre-trained Neural Networks

David Chayem Abdou, Faten Fadia Mohamed

Publication Year: 2019, Page(s) 306 - 310

Cited by: Papers (4)

Abstract HTML

Design and Analysis of Fractional-order Oscillators Using Bolya

Khalid Singh, Pradip Kumar, Mohd Noh Karim, Sabo Miya Hassan, Immanuel Esmailzadeh, Arun Muthu Dhan

Publication Year: 2019, Page(s) 311 - 316

Cited by: Papers (5)

Abstract HTML

Data Clustering Technique for In-Network Data Reduction in Wireless Sensor Network

M.K. Abeer, Azzine Abd Aziz, S.A. Laif, Azzine Azzam

Publication Year: 2019, Page(s) 317 - 322

Cited by: Papers (4)

Abstract HTML

EEG Data Compression using Truncated Singular Value Decomposition for Remote Driver Status Monitoring

M.K. Abeer, Azzine Abd Aziz, S.A. Laif, Azzine Azzam

Publication Year: 2019, Page(s) 323 - 327

Cited by: Papers (4)

Abstract HTML

Remote Monitoring of Coupled Tank Accompanied by PLC-OPC-MATLAB Architecture

Isahar Shekharwar, Rajan Chilo, Sumit Arora, Immanuel Esmailzadeh

Publication Year: 2019, Page(s) 328 - 332

Cited by: Papers (1)

Abstract HTML

Multi-Agent Based Energy Management in Microgrids Using MAC-BMIX

Upasana Lakshmi, I. Esmailzadeh, Naveen Badraddin, P. Marudavean, G. Hameed, Ajay Jangra

Publication Year: 2019, Page(s) 333 - 338
















Abstract HTML

**Need Full-Text**  
access to IEEE Xplore for your organization?  
[CONTACT IEEE TO SUBSCRIBE](#)

**10 YEARS**  
IEEE Access is celebrating its 10 Year Publishing Anniversary!  
View the top 10 articles published over the last decade based on downloads, citations, and overall impact in IEEE Xplore of interest.  
[View Articles](#)



---

<input type="checkbox"/>	<b>Feature selection of Human Daily Activities using Ensemble method Classification</b>	
	Ku Natharini, I. Elasmouh, L.I. Ishaq, Ghazi Capri Publication Year: 2019, Page(s) 339 - 344 Cited by: Papers (3)	
	Abstract HTML  	
<hr/>		
<input type="checkbox"/>	<b>Classification of Rheumatoid Arthritis using Machine Learning Algorithms</b>	
	Ho Sharon, I. Elasmouh, CK. Lu, S. Panchanathan, Eranjo Natarajan Publication Year: 2019, Page(s) 245 - 250 Cited by: Papers (8)	
	Abstract HTML  	
<hr/>		
<input type="checkbox"/>	<b>Author Index</b>	
	Publication Year: 2019, Page(s) 31 - 37  	
<hr/>		
<input type="checkbox"/>	<b>Table of contents</b>	
	Publication Year: 2019, Page(s) 8 - 8  	
<hr/>		
<input type="checkbox"/>	<b>List of Reviewers</b>	
	Publication Year: 2019, Page(s) 18 - 18  	

---

## **Effect of various repetition coating and thickness of YSB electrolyte on the electrochemical performance of the single button cell solid oxide fuel cell**

Dedikarni Panuh <sup>a,c\*</sup>, Dody Yulianto <sup>a</sup>, M. F. Shukur <sup>b</sup>, Andanastuti Muchtar <sup>a</sup>,

<sup>a</sup>Department of Mechanical Engineering, Faculty of Engineering, Universitas Islam Riau, Indonesia

<sup>b</sup>Fundamental and Applied Sciences Department Universiti Teknologi Petronas, Seri Iskandar, Malaysia

<sup>c</sup>Fuel Cell Institute, Universiti Kebangsaan Malaysia, 43600 UKM Bangi, Selangor, Malaysia

\*Corresponding Author: dedikarni@eng.uir.ac.id

### **ABSTRACT**

Reducing the operating temperature and optimization design while maintaining high cell performance is the primary consideration in designing current SOFCs. The effect of the electrolyte YSB thickness on the electrochemical performance of the single cell was measured from 500–650°C was studied in detail. Cell performance testing was performed using impedance for electrochemical characterization and single-cell capability testing. The YSB electrolyte coated on the NiO–SDC | SDC substrates was deposited as a thin film with varying thicknesses of 1.5, 3.5, 5.5, and 7.5 µm after 1, 2, 3, and 4 applications of coatings, respectively, at a sintering temperature of 800°C for two h. These findings confirmed that the number of layers was proportional to the thickness of the YSB electrolyte. The results indicated that the bilayer electrolyte system of  $Y_{0.25}Bi_{0.75}O_{1.5}/Sm_{0.2}Ce_{0.8}O_{1.90}$  with three applications of coating at 650°C exhibited optimum current and power densities of 228 mA/cm<sup>2</sup> and 82 mW/cm<sup>2</sup>, respectively. The interfacial polarization cells achieved a low total resistance (0.55 Ωcm<sup>2</sup>) and a high open circuit potential (1.092 V) after three coating applications with 5–6 µm thickness at 600°C. This study produced a single button cell system with a total deficient cell interfacial resistance compared to the previous studies on intermediate and low-temperature SOFCs.

**Key Words:** SOFC, Bilayer Electrolyte, SDC, YSB.

## Introduction

High operating temperature is one of the main barriers to the wide-scale adoption of solid oxide fuel cell (SOFC) technology [1]. Therefore, most research focused on developing low-intermediate temperature SOFC operating at around range temperature 500-600 [2]. To achieve low-intermediate temperatures, several from the viewpoint of new materials, novel processes, and unique architectures must be re-examined [3].

Recently most research and development activities on SOFC are mainly focused on the commercially viable SOFC manufacturing technology with high electrochemical performance, the transformation of stack design, and cost-effective process. In fabrications, p has been proposed and developed for SOFC. Various are available for depositing films on dense or porous substrates based on ceramic powder techniques or chemical and physical processes. These methods include electrochemical vapor deposition, chemical vapor deposition, physical vapor deposition (radio frequency and magnetron sputtering), laser ablation, plasma spraying, and depositing techniques [4][5].

Although the methods mentioned above are well established, the investment cost for the apparatus is higher than those used in the dip coating method. Dip coating is expected to produce a satisfactory surface condition in the fabrication of YSB bilayered composite film electrolyte on the SDC electrolyte because the thickness of the electrolyte substrate can be easily controlled through the number of dip coatings. This technique is the simplest and the most appropriate method for preparing films with large surface areas [6]. Furthermore, dip coating is inexpensive and more suitable for mass production, even in multi-layer cells.

Electrolyte thickness is essential and must be considered because surface morphology has a vital function in the physical and chemical properties of the bilayer electrolyte [7][8]. However, details of the optimum thickness and electrochemical properties of YSB composite electrolytes on SDC/YSB bilayered electrolytes are scarce. This study aims to determine the influence of SDC/YSB bilayered combined electrolyte thickness on the interfacial polarization resistance and electrochemical performance of single SOFC cells with SDC/YSB as a bilayered electrolyte, Ag-YSB composite as cathode and NiO–SDC as an anode.

## Experiment Procedure

### 2.1 Materials and specimen preparation

Commercial material available yttrium oxide (99.999 wt%) and bismuth (III) oxide (99.999 wt%, Sigma Aldrich Sdn. Bhd) was mixed at a molar ratio 1 of : 3. The powder and Zirconia ball (Fritsch Pulverisette 6) in ethanol was combined with mechanical mill method for 24 h, and then calcined in air at 750 °C. This-gel practice prepares three-element SDC powder with (Ce<sub>0.8</sub>sol-gel<sub>1.9</sub>) d [9].

NiO, Nickel (II) Oxide (99.8 wt%, Sigma Aldrich Sdn. Bhd), and SDC powder were mixed at a weight ratio of 60:40 and were prepared by ball milling in ethanol for 24 h. NiO-SDC powers were mixed with zirconia ball medium, dried in an oven at 80 °C for 12 h, and thoroughly ground. The dried powders were then heated and called at 1100°C for 5 hours to obtain NiO-SDC composite powder.

To prepare the Ag-YSB cathode slurry, silver (I) oxide (99.8 wt%, Sigma Aldrich Sdn. Bhd) and YSB were added at a weight ratio of 50:50. The  $\alpha$ -terpineol, di-n-butyl phthalate (Merck Sdn. Bhd), and polyvinyl butyral (PVB) (Sigma) as organics binder were mixed at a volume ratio 3: 1: 2. The organics binder was ma mixture with agate mortar in ethanol as a dispersing medium for 30 min.

### 2.2 Characterization

The microstructure of single button cells SOFC samples was observed using field emission scanning electron microscopy (FESEM), and the formation of different phases by the Ag-YSB, YSB, SDC, and NiO/SDC system during the coating of bilayer electrolyte films was investigated using X-ray diffraction (XRD) and electrochemical impedance spectroscopy (EIS). The temperature and mass loss with phase transformation was determined by gravimetric analysis and differential scanning calorimetry (TGA and DSC Jupiter 449F3) from 30 °C to 1200 °C. The phase of the cathode was analyzed using XRD (semen D-500) with Cu K $\alpha$  at a 2 $\theta$  range from an angle of 20° to 80°, and the Rietveld method using the EVA software were obtained pattern refinements. The morphology and grain size of the composite cathode pellets was observed using a Scanning electron microscope (Zeiss EVA MA10) with 15 XK magnification.

### 2.3 Button single-cell fabrication, performance, and electrochemical measurement

The NiO-SDC anode and the SDC electrolyte pellets were co-pressing by cold pressing. The pellet was used as a substrate or half-cell (25 mm diameter and sintered at 1400°C for five h). The NiO-SDC anode and SDC/YSB bilayered electrolyte (half Cell) were coated with Ag-YSB cathode slurry using SPM. The  $\text{Ag}_2\text{O}_3$  and YSB powder as composite cathode and organic binder were mixed by SPM, then deposited onto the substrate surface. The slurry containing the composite and organic binder desired to make the solid deposited film by a chemical reaction method. And then, the influence of the coating process on thickness layers was investigated with four times repetitions. By sintering, the composite cathode fabricates at 800 °C for two h in air. The complete single SOFC button cell system became the end product system. The final configuration button single cell (NiO-SDC/SDC/YSB/Ag-YSB) based on substrate SDC/YSB as a bilayer electrolyte is shown in fig 1.

The half cell with Ag-YSB composite cathode was measured electrochemical performance (interfacial polarization resistance,  $R_p$ ) using EIS Autolab Nova 1.8 Model PGSTAT302N). The impression of repetition of coating and temperature on cell performance was assessed using impedance spectroscopy. This test has been widely used to determine the achievements of solid oxide fuel cells involving more complex curvature (arc) with various processes and materials used in making single cells. Different cell manufacturing processes have contributed to a more complex impedance spectrum. The impedance spectrum has been used to separate and identify the bulk interfacial polarization resistance ( $R_p$  Total, Report), the constant phase element (CPE), and the interfacial polarization resistance ( $R_p$ ) in the range of 0.01 Hz to 10 kHz.

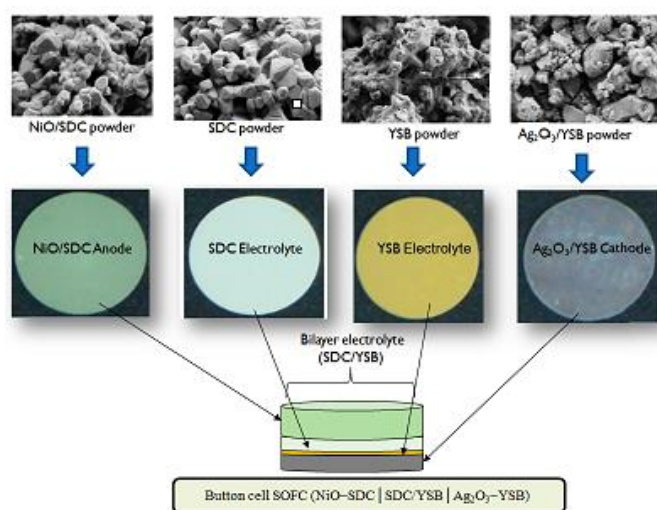


Fig. 1 A schematic configuration of NiO-SDC/SDC/YSB/Ag-YSB as a button

single cell SOFC.

## 4. Result and discussion

### 4.1 Button Single-Cell Performance Analysis

The performance of cells is shown in Figure 2, with hydrogen and pure oxygen as oxides. Performance measurements were performed at operating temperatures of 600°C.

Studies on the effect of YSB electrolyte thickness on the surface of the SDC electrolyte in the form of NiO–SDC | SDC/YSB | Ag<sub>2</sub>O<sub>3</sub>–YSB single cell. NiO–SDC anode is a supporting substrate, and Ag<sub>2</sub>O<sub>3</sub>–YSB is a cathode. The current density and voltage (I-V) performance on YSB thickness was conducted with NiO–SDC | SDC/YSB | Ag<sub>2</sub>O<sub>3</sub>–YSB single-cell anode support. YSB electrolyte performance testing can be performed when a cell is designed with SDC electrolyte on the anode surface, and YSB is coated on the cathode surface to stabilize YSB and SDC under oxygen reduction ( $P_{O_2}$ ) conditions [10][11].

The results of the performance tests of open-circuit potential (OCP), current density (I), and power density (P) of cells at 600°C are shown in Figure 2 (a). The maximum power density of a single cell NiO–SDC | SDC/YSB | Ag<sub>2</sub>O<sub>3</sub>–YSB with a single YSB electrolyte coating was 66.1 mW/cm<sup>2</sup>, and the maximum current density was 188 mA/cm<sup>2</sup> at 600°C.

The result of the measurement of the maximum power density in the second YSB electrolyte coating with a yield of 72 mW/cm<sup>2</sup> and the maximum current thickness was 212.2 mA/cm<sup>2</sup> as shown in Figure 2 (b). Figure 2 (c) shows the results of the measurement of maximum power density during the third YSB electrolyte coating of 82 mW/cm<sup>2</sup> and maximum current thickness with yields of 225.3 mA/cm<sup>2</sup>. Figure 2 (d) shows the results of measuring the maximum power density at four times the YSB electrolyte coating is 80 mW/cm<sup>2</sup> and the maximum current density is 218.7 mA/cm<sup>2</sup>. Increased OCP (Volt), I (mA/cm<sup>2</sup>), and P (mW/cm<sup>2</sup>) values from one coating to the fourth coating, as shown in Figure 2. The maximum power density was obtained at an operating temperature of 600°C with an average electrolyte thickness (YSB) of 5.5 μm, which was the third time. Subsequently, OCP, I-V, power density, and ty values began declining during the fourth coating. In parallel with the FESEM thickness test, four coating times produced YSB electrolyte thickness at an average thickness of 7.5 μm. The effect of increasing the number of coatings on the OCP value, current density, and single-cell power developed is shown in Figure 2. The maximum voltage value, power density, and present are obtained by optimizing the YSB electrolyte thickness value. The increase in V

(Volt),  $I$  ( $\text{mA}/\text{cm}^2$ ), and  $P$  ( $\text{mW}/\text{cm}^2$ ) values of the YSB electrolyte thickness change is evidence that YSB electrolytes have successfully inhibited electrolyte conductivity (SDC) since the reduction of  $\text{Ce}^{4+}$  to  $\text{Ce}^{3+}$  did not occur in the interface area so that it does not affect cell performance. Increased voltage, current, and power values are also observed in ESB/GDC double-layer thin film electrolytes [12]. Ahn et al. (2009) [12] reported that ESB thin film electrolytes were produced on the surface of GDC electrolytes using a physical vapor deposition (PVD) method. Ahn et al. (2009) also reported that the performance of single button cells with double-layer electrolyte thin film (ESB/GDC) film ( $\sim 10 / \sim 4 \mu\text{m}$ ) resulted in an OCP increase of 0.72 to 0.77 V.

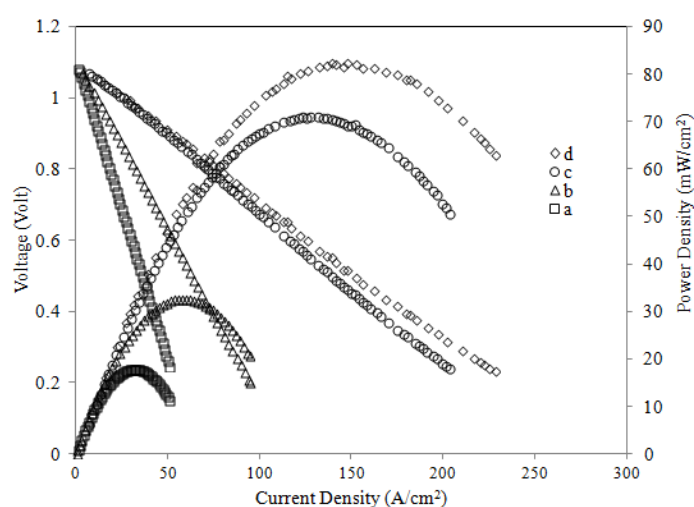


Figure 2 Current ( $I$ ) –Voltage ( $V$ ) performance test with (a) one, (b) two, (c) three, (d) four YSB coating times the bilayer electrolyte

The average OCP for various repeats of YSB electrolyte coating on the surface of the SDC electrolyte is shown in Figure 3. OCP values in one coating up to four times coating are 1.068 V, 1.072 V, 1.092 V, and 1.084 V. OCP, I-V values, and optimum power density are in the third coating with moderate operating temperature ( $600 \text{ }^\circ\text{C}$ ) with OCP value of 1.092 V, a current density of  $0.23 \text{ mA}/\text{cm}^2$  and a power density of  $82 \text{ mW}/\text{cm}^2$ . Increasing the number of coatings up to three repetitions increased the OCP value to 1.092 V. The optimum coating thickness was performed three times to repeat the YSB electrolyte coating on the surface of the SDC electrolyte and produced a YSB electrolyte thickness of  $5.5 \mu\text{m}$ . Increased OCP value, up to 1.092 V, current density  $0.23 \text{ mA}/\text{cm}^2$  and power density  $82 \text{ mW}/\text{cm}^2$ . The SDC, in this case, produced an oxygen vacancy in which three  $\text{O}^{2-}$  ions replaced four  $\text{O}^2$  ions. The emptiness

of the oxygen site has led to the movement of electrons and the increase in ion flow in the electrolyte. SDC is a highly ionic conductivity material with a readily available oxygen atom in which the movement causes ion flow.

Optimum coating and thickness have resulted in maximum OCP value. However, the fourth coating decreased the OCP value to 1.084 V. Increasing the thickness to 7.5  $\mu\text{m}$  in the fourth coating decreased the OCP value. This condition occurs when the YSB electrolyte thickness exceeds the optimum thickness, and the YSB electrolyte begins to decompose. In SDC electrolytes,  $\text{Ce}^{4+}$  to  $\text{Ce}^{3+}$  electrons were decreased at low oxygen partial pressure and mixing of ion and electron conductance. Mixing electrons and ions with high-performance electrolytes has led to short circuits and decreased cell performance. YSB electrolyte thin films can prevent the cell from degrading and inhibiting electrolyte conductance across the electrolyte. YSB electrolytes are used to suppress electron conductivity from the substrate, and YSB thin layers are also used to produce high ion conductance. The SDC layer acts as a support for the YSB to be stable and stable [13].

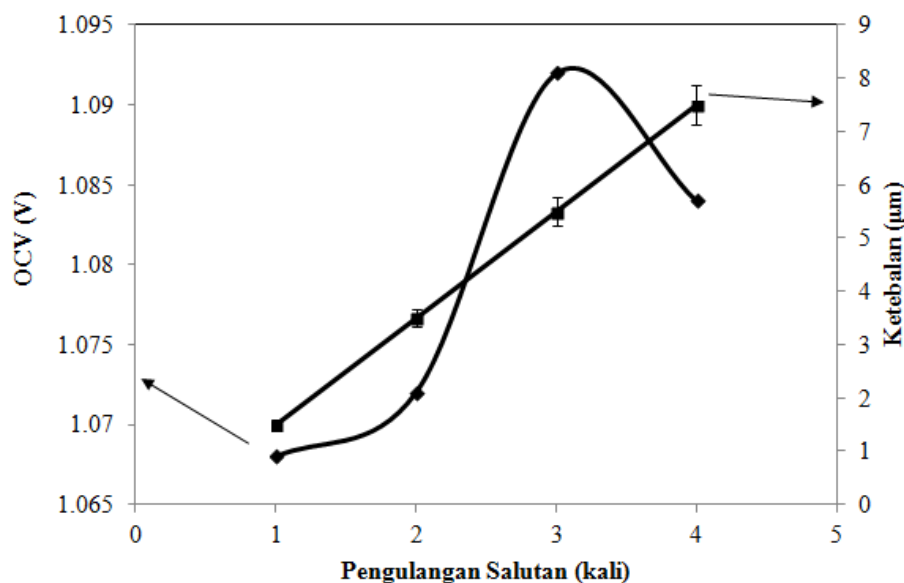


Figure 3 Average OCP for various repetition coating and thickness of YSB electrolyte on SDC electrolyte surface

Bilayer electrolyte analysis for YSB / SDC has also been investigated by Virkar (1991) [14], Huang et al. (2008) [15], and Zhang et al. (2011) [13]. Oxygen partial pressure ( $P_{O_2}$ ) values of two electrolytes were determined by the electrolyte thickness ratio and ion and electron conductivity of both electrolytes. The use of thin layers of SDC  $<10 \mu\text{m}$  and YSB  $<6 \mu\text{m}$  gave a low resistance drop and provided control to the surface for no degradation. This is because the oxygen partial pressure ( $P_{O_2}$ ) interfacial with the SDC is further. The thickness of



YSB  $<6 \mu\text{m}$  and SDC  $<10 \mu\text{m}$  protected the electrolyte in bulk. However, if a very thick YSB film is found, it can increase the electrolyte resistance and cause a decrease in ion conductivity. YSB electrolyte films that are too thick also make YSB easy to decompose. This is due to the oxygen partial pressure ( $P_{O_2}$ ) and the rising temperature of the environment.

#### 4.2 Impedance spectroscopy analysis

Four impedance spectra with one repetition of the coating to four times the layer, as shown in Figure 4. Each repetition of the coating consists of three overlapping arcs. Figure 4 (a) shows the impedance spectrum with one coating. Three turns in the figure with a larger diameter than the YSB electrolyte as a second coating. This condition indicates a more significant overall coating than the second YSB electrolyte coating. Figure 4 (b) shows the impedance spectrum with twice the layer. The figure showed three arcs with smaller diameters than the YSB electrolyte coating for the first repetition and more significant than the third coating.

This phenomenon shows that the overall resistance in the second coating is smaller than the one coating, and the thick one is the YSB electrolyte coating a third time. Figure 4 (c) shows the impedance spectrum with three times the layer. The figure showed three half rounds with smaller diameters than all YSB electrolyte coatings. This condition applies because three times, the coating is sufficient to cover the entire surface of the SDC electrolyte with the optimum coating thickness and gives the lowest overall resistance; Rajah 4 (d) shows the impedance spectrum with four times the YSB electrolyte coating on the SDC surface. Impedance spectrum at one time coating so that four times the coating exhibited a decrease in half size and increased initially at the fourth time coating. This phenomenon holds because the increase in layer gives the impression of decreasing the overall barrier of cells so that optimum thickness is achieved. This condition is indicated by the decrease in size halfway around between the third coating is more closely matched so that it overlaps on the bulk resistance ( $R_b$ ) and the electrode resistance ( $R_e$ ), and the repetition of the layer has reached the optimum thickness three times to produce a decrease in minimum resistance. However, the overall resistance has reincreased for the fourth time. This condition is shown by the enlargement of half the size of the electrode resistance ( $R_e$ ).

The first arc for a real axis at high frequencies is the ohm resistance ( $R_s$ ) contributed by the wire and cell resistance. In this study, the platinum mode is connected to the outer circuit to determine the value of resistance, OCP, power, and current density. Interfacial polarization resistance ( $R_p$ ),  $R_p$  is the bulk resistance ( $R_{\text{bulk}}$ ,  $R_b$ ) + grain boundary resistance ( $R_{\text{grain}}$ ),

$R_g$ ) + resistance electrode ( $R_{\text{elektrode}}$ ,  $R_e$ ), and the total polarization resistance ( $R_{\text{report}}$ ) is  $R_s + R_p$ . All these resistance are known to use Autolab with Nova 1.5 software in the form of equal spectra and circuits to obtain the value of each coated resistance.

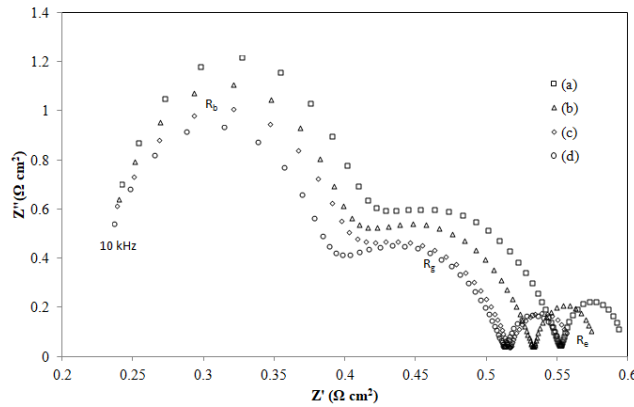


Figure 4 The impedance spectrum shows the variety of coating repetitions: (a) once, (b) twice, (c) three times, and (d) four times.

The impedance spectral equivalent circuit of SOFC single button cells with YSB electrolyte thickness at one time repeated coating up to four times with coating resistance total ( $R_{\text{report}}$ ),  $0.6 \Omega\text{cm}^2$ ,  $0.56 \Omega\text{cm}^2$ ,  $0.55 \Omega\text{cm}^2$  and  $0.58 \Omega\text{cm}^2$  and interfacial resistance ( $R_p$ )  $0.37 \Omega\text{cm}^2$ ,  $0.34 \Omega\text{cm}^2$ ,  $0.33 \Omega\text{cm}^2$ ,  $0.35 \Omega\text{cm}^2$  as shown in Figure 5 and 6. However, different electrolyte layer thicknesses do not have a significant impact on the ohm resistance ( $R_s$ ) values of  $0.228 \Omega\text{cm}^2$ ,  $0.225 \Omega\text{cm}^2$ ,  $0.224 \Omega\text{cm}^2$  and  $0.227 \Omega\text{cm}^2$  as the ohm resistance value is related to the interconnect wire between the cell and the outer circuit. In this study, the value of the ohm resistance has little effect on the overall resistance and can be ignored because the same connection wire is used every time a test is used. Therefore, modification of the ohm resistance is unnecessary as it does not significantly impact the system as a whole.

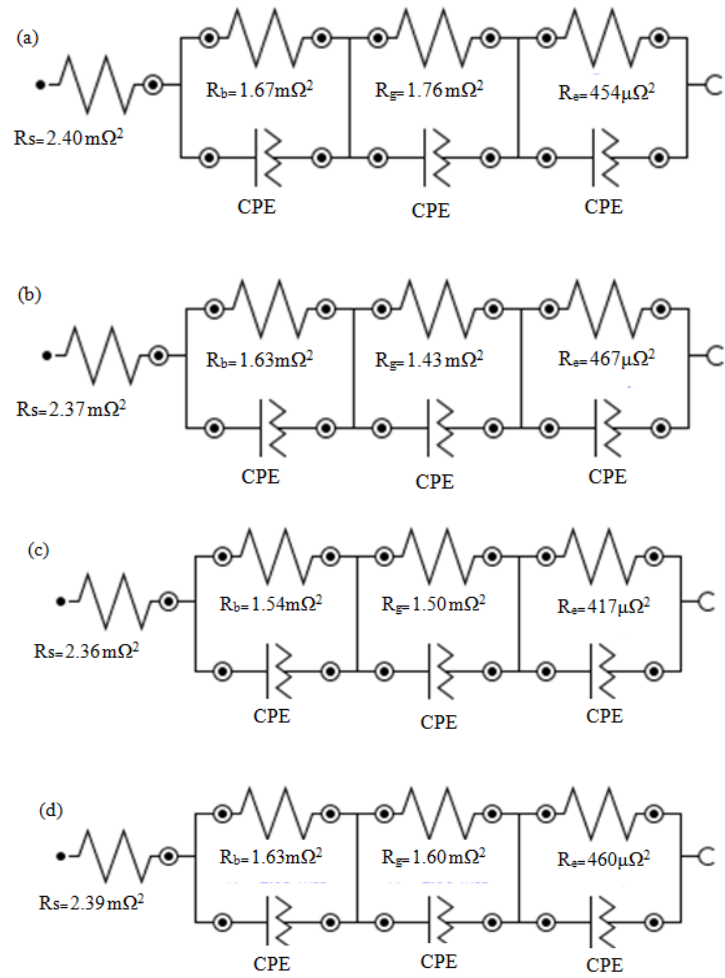


Figure 5 Impedance spectrum equivalent circuits based on various coating repetitions: (a) once, (b) twice, (c) three times, and (d) four times.

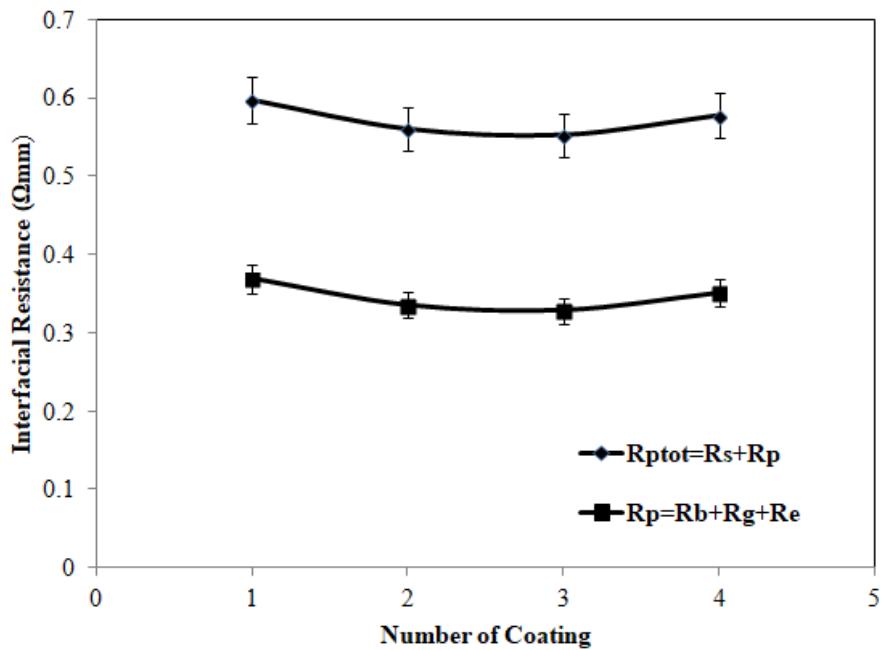


Figure 6 Total interfacial polarization resistance ( $R_{p_{tot}}$ ) and bulk interface polarization resistance ( $R_p$ ) at various coating repetitions: (a) once, (b) twice, (c) three times, and (d) four times.

The addition of the YSB electrolyte coating up to 4 times reduced the interfacial resistance value ( $R_p$ ) contributed by the grain resistance (Rebound,  $R_g$ ) and the electrode resistance (Relectrode,  $R_e$ ). YSB electrolyte coating produced a  $0.60 \Omega\text{cm}^2$  polishing interfacial and dropped to  $0.55 \Omega\text{cm}^2$  on the third coating. The third coating with a thickness of  $5.5 \mu\text{m}$  gave the lowest  $R_p$  value, and the interface resistance increased again to  $0.58 \Omega\text{cm}^2$  on the fourth coating. The addition of YSB electrolyte coating on the surface of the SDC electrolyte affected the interfacial polarization resistance ( $R_p$ ). The three-coating addition of YSB electrolyte coating reduced the opposition to a minimum because the third coating successfully thinned the entire surface of the SDC electrolyte and prevented the flow of electrons from the SDC electrolyte ideally. Two-layer electrolyte analysis for YSB/SDC was also studied by Virkar (1991)[14], Huang et al. (2008)[15], and Zhang et al. (2011) [13].

The oxygen partial pressure ( $P_{O_2}$ ) of two electrolytes is determined by the ratio of electrolyte thickness and ion and electron conductivity of both electrolytes. The thickness of YSB  $< 2 \mu\text{m}$  protected the electrolyte in bulk, and the  $\text{CeO}_3/\text{YSB}$  thickness ratio was large. If the oxygen partial pressure ( $P_{O_2}$ ) interface is too close to the surface and the YSB film is insufficient to cover the ceria surface, then there is a decrease in the shear due to exposure to  $P_{O_2}$ . The use of a thin layer of fiber ( $< 10 \mu\text{m}$ ) with a YSB thin layer of  $< 6 \mu\text{m}$  gave a decreasing resistance and showed the control of the ceria no reduction, as the oxygen partial pressure ( $P_{O_2}$ ) interfacial was closer to the fuel. However, adding up to four times the coating exceeds the maximum threshold, resulting in an increase in the polarization resistance of the interfacial. Excessive growth in the number of layers can also prevent the flow of electrons and ion conductance from the electrolyte to the cathode.

This decrease in the interfacial polarization resistance is due to the maximum ability of the YSB electrolyte to inhibit the conductivity of the SDC electrons across the YSB electrolyte. It is expected to increase the conductivity of the oxygen ions across the YSB electrolyte. The decreased  $R_p$  was also due to the compatibility between the YSB electrolyte and the  $\text{Ag}_2\text{O}_3$ -YSB cathode. Using the same electrolyte and electrode materials is expected to facilitate the conductivity of oxygen ions from electrolytes with YSB material and cathode composites with YSB and  $\text{Ag}_2\text{O}_3$  mixtures. According to the report of Zhang et al. (2010)[16] and Kenjo and

Kanehira (2002)[17], this phenomenon also occurs in LSM–YSB materials and YSB electrolytes. The decrease in  $R_p$  is due to the increase in oxygen ion conductance and chemical compatibility between the cathode material (LSM–YSB) and the YSB electrolyte. Chemical compatibility between cathode and electrolyte occurs when electrolytes and cathodes are based on the same material until the manufacture and operation of a single button cell do not occur, cracking and separation of each component due to different thermal expansion. Low and high-frequency intervals for interfacial polarization resistance ( $R_p$ ) are also contributed by the anode and cathode [18]. In this study, the high frequency (1 kHz) and low (0.1 Hz) shortcuts occur on the Z' axis approaching  $0.4 \Omega\text{cm}^2$ .

The results of this study are compared to several previous studies with SDC/YSB bilayer-layer electrolytes at 0.5 mm SDC thickness and 5.5  $\mu\text{m}$  YSB and  $\text{Ag}_2\text{O}_3$ /YSB cathode material with an operating temperature of 600 °C as shown in Table 4.2. This study using YSB electrolyte materials yielded higher OCP results than previous research. Previous research reports by Wachsman et al. (1992) [19] on GDC/ESB bilayer-layer electrolytes at 0.9  $\mu\text{m}$  GDC thickness and 50-60  $\mu\text{m}$  ESB thickness with Au cathode materials gave an OCP value of up to 0.901-0.977 V. This is due to the unstable ceria and the use of Au as a cathode material as a good electron conductor

Park and Wachsman (2006)[20] investigated the SDC/ESB bilayer layer electrolyte at 1.5  $\mu\text{m}$  SDC thickness and nine  $\mu\text{m}$  ESB with Au cathode material, giving OCP value up to 0.783 V. And then, Park and Wachsman (2006) investigated the SDC/ESB bilayer layer electrolyte at thickness 1.5  $\mu\text{m}$  SDC and 22  $\mu\text{m}$  ESB with Ag/YSB cathode material gave an OCP value of up to 0.949 V. The increase in ESB electrolyte thickness on the SDC surface resulted in an increase in OCP value from 0.783-0.949 V. The OCP value increase occurred due to the ESB increasing ion conductivity and did not occur because the SDC backing electrolyte successfully prevented YSB from decomposition.

Leng and Chan (2006) [21] investigated the bilayer-layer GDC/YSB electrolyte at GDC thickness of 84  $\mu\text{m}$  and YSB 6  $\mu\text{m}$  with Pt cathode material giving an OCP value of up to 0.885 V. Zhang et al. (2010) [16] investigated the bilayer-layer SDC/YSB electrolyte at SDC 26 and 6  $\mu\text{m}$  thickness with LSM / YSB cathode material giving OCP values up to 0.897 V and Zhang et al. (2011)[13] investigated the bilayer-electrolyte at GDC/YSB thickness with GDC thickness of 26  $\mu\text{m}$  and YSB 6  $\mu\text{m}$  with Ag/YSB cathode material giving OCP value of up to

0.887 V. OCP value increase occurred in the event of a decrease in the support electrolyte thickness. This is due to the reduction of the supporting electrolyte thickness, which increases the conductivity of the ion from the cathode to the electrolyte. However, the use of not match electrolyte cathode material reduced the OCP value from 0.897-0.887 V. This is due to electrolyte material that does not fit the cathode and causes both components to not optimally, thus reducing cell performance. Therefore, it can be concluded that the performance value differences from some previous studies were due to different material selection parameters, manufacturing methods, and coating thickness. Optimization of material selection parameters, manufacturing methods, and coating thickness also contributed to the increased OCP value.

#### 4 CONCLUSIONS

The  $Y_{0.25}Bi_{0.75}O_{1.5}$  electrolyte (YSB) was used to suppress the electron conductivity of the substrate, and the YSB thin layer (5.5  $\mu\text{m}$ ) was used to produce high conductivity in the electrolyte. The YSB thin film electrolyte coating on the surface of the SDC electrolyte prevented  $Ce_2O_3$  from being exposed to partial oxygen pressure. Increased OCP value, up to 1.092 V, current density 0.23  $\text{mA}/\text{cm}^2$  and power density 82  $\text{mW}/\text{cm}^2$ . The SDC, in this case, produced an oxygen vacancy in which three  $O^{2-}$  replaced four  $O^2$  ions. The emptiness of the oxygen site has led to the movement of electrons and the increase in ion flow in the electrolyte. The YSB with the  $Y_{0.25}Bi_{0.75}O_{1.5}$  system prevented the ceria ( $Ce_2O_3$ ) from degrading ( $Ce^{4+}$  to  $Ce^{3+}$ ) and restricted the electrons' conductivity across the electrolyte. The thick (0.5 mm) SDC layer acts as a YSB support for more OCP and stability single button solid oxide fuel cell.

#### ACKNOWLEDGMENTS

The author acknowledges Universiti Petronas Malaysia, the Universitas Islam Riau, for the matching grand research sponsorship under Nomor: 468/Kontrak/LPM-UIR-9-2018 and 361/Kontrak/LPPM-UIR/4-2018.

#### REFERENCES

- [1] S. P. S. Badwal and K. Foger, "Solid Oxide Electrolyte," *Ceram. Int.*, vol. 8842, no. 95, pp. 257–265, 1996.
- [2] K. Eguchi, T. Setoguchi, T. Inoue, and H. Arai, "Electrical properties of ceria-based oxides and their application to solid oxide fuel cells," *Solid State Ionics*, 1992.
- [3] D. Yang *et al.*, "Low-temperature solid oxide fuel cells with pulsed laser deposited bi-

- layer electrolyte,” *J. Power Sources*, 2007.
- [4] Y. C. Yang, P. H. Wang, Y. T. Tsai, and H. C. Ong, “Influences of feedstock and plasma spraying parameters on the fabrication of tubular solid oxide fuel cell anodes,” *Ceram. Int.*, 2018.
- [5] L. S. Wang, C. X. Li, C. J. Li, and G. J. Yang, “Performance of La<sub>0.8</sub>Sr<sub>0.2</sub>Ga<sub>0.8</sub>Mg<sub>0.2</sub>O<sub>3</sub>-based SOFCs with atmospheric plasma sprayed La-doped CeO<sub>2</sub> buffer layer,” *Electrochim. Acta*, 2018.
- [6] D. Panuh, A. Muchtar, N. Muhamad, E. H. Majlan, and W. R. W. Daud, “Fabrication of thin Ag-YSB composite cathode film for intermediate- temperature solid oxide fuel cells,” *Compos. Part B Eng.*, 2014.
- [7] T. Talebi, M. Haji, and B. Raissi, “Effect of sintering temperature on the microstructure, roughness and electrochemical impedance of electrophoretically deposited YSZ electrolyte for SOFCs,” in *International Journal of Hydrogen Energy*, 2010.
- [8] M. S. Djošić, V. B. Miskovic-Stankovic, and V. V. Srdić, “Electrophoretic deposition and thermal treatment of boehmite coatings on titanium,” *J. Serbian Chem. Soc.*, vol. 72, no. 3, pp. 275–287, 2007.
- [9] A. Bodén, J. Di, C. Lagergren, G. Lindbergh, and C. Y. Wang, “Conductivity of SDC and (Li/Na)<sub>2</sub>CO<sub>3</sub> composite electrolytes in reducing and oxidizing atmospheres,” *J. Power Sources*, vol. 172, no. 2, pp. 520–529, 2007.
- [10] T. Takahashi, T. Esaka, and H. Iwahara, “Conduction in Bi<sub>2</sub>O<sub>3</sub>-based oxide ion conductor under low oxygen pressure. II. Determination of the partial electronic conductivity,” *J. Appl. Electrochem.*, vol. 7, no. 4, pp. 303–308, 1977.
- [11] N. Jiang, E. D. Wachsman, and S. H. Jung, “A higher conductivity Bi<sub>2</sub>O<sub>3</sub>-based electrolyte,” *Solid State Ionics*, vol. 150, no. 3–4, pp. 347–353, 2002.
- [12] J. S. Ahn *et al.*, “High-performance bilayered electrolyte intermediate temperature solid oxide fuel cells,” *Electrochem. Commun.*, vol. 11, no. 7, pp. 1504–1507, 2009.
- [13] L. Zhang, L. Li, F. Zhao, F. Chen, and C. Xia, “Sm<sub>0.2</sub>Ce<sub>0.8</sub>O<sub>1.9</sub>/Y<sub>0.25</sub>Bi<sub>0.75</sub>O<sub>1.5</sub> bilayered electrolytes for low-temperature SOFCs with Ag-Y<sub>0.25</sub>Bi<sub>0.75</sub>O<sub>1.5</sub> composite cathodes,” *Solid State Ionics*, vol. 192, no. 1, pp. 557–560, 2011.
- [14] A. V. Virkar, “Theoretical analysis of solid oxide fuel cells with two-layer, composite electrolytes: Electrolyte stability,” *J. Electrochem. Soc.*, vol. 138, no. 5, pp. 1481–1487, 1991.
- [15] S. Huang, G. Zhou, and Y. Xie, “Electrochemical performances of Ag-

- (Bi<sub>2</sub>O<sub>3</sub>)<sub>0.75</sub>(Y<sub>2</sub>O<sub>3</sub>)<sub>0.25</sub> composite cathodes,” *J. Alloys Compd.*, vol. 464, no. 1–2, pp. 322–326, 2008.
- [16] L. Zhang, C. Xia, F. Zhao, and F. Chen, “Thin film ceria-bismuth bilayer electrolytes for intermediate temperature solid oxide fuel cells with La<sub>0.85</sub>Sr<sub>0.15</sub>MnO<sub>3-δ</sub>-Y<sub>0.25</sub>Bi<sub>0.75</sub>O<sub>1.5</sub> cathodes,” *Mater. Res. Bull.*, vol. 45, no. 5, pp. 603–608, 2010.
- [17] T. Kenjo and Y. Kanehira, “Influence of the local variation of the polarization resistance on SOFC cathodes,” *Solid State Ionics*, vol. 148, no. 1–2, pp. 1–14, 2002.
- [18] S. Zha, Y. Zhang, and M. Liu, “Functionally graded cathodes fabricated by sol-gel/slurry coating for honeycomb SOFCs,” *Solid State Ionics*, vol. 176, no. 1–2, pp. 25–31, 2005.
- [19] E. D. Wachsman, G. R. Ball, N. Jiang, and D. A. Stevenson, “Structural and defect studies in solid oxide electrolytes,” *Solid State Ionics*, vol. 52, no. 1–3, pp. 213–218, 1992.
- [20] J. Y. Park and E. D. Wachsman, “Stable and high conductivity ceria/bismuth oxide bilayer electrolytes for lower temperature solid oxide fuel cells,” *Ionics (Kiel)*, vol. 12, no. 1, pp. 15–20, 2006.
- [21] Y. J. Leng and S. H. Chan, “Anode-supported SOFCs with Y<sub>2</sub>O<sub>3</sub>-doped Bi<sub>2</sub>O<sub>3</sub>/Gd<sub>2</sub>O<sub>3</sub>-Doped CeO<sub>2</sub> composite electrolyte film,” *Electrochem. Solid-State Lett.*, vol. 9, no. 2, pp. 10–14, 2006.





UNIVERSITI  
TEKNOLOGI  
PETRONAS

# CERTIFICATE

\_\_\_\_\_ of presenter \_\_\_\_\_

This is to certify that

**DR DEDIKARNI**

has participated in

**INTERNATIONAL SEMINAR ON UTP - UIR  
MATCHING GRANT PROGRESS REPORT 2019**

on

**11<sup>TH</sup> & 12<sup>TH</sup> MARCH 2019**

at

**UNIVERSITI TEKNOLOGI PETRONAS**

organized by

**FUNDAMENTAL & APPLIED SCIENCES  
DEPARTMENT (FASD)**

**ASSOC. PROF. DR. HANITA BT DAUD**  
Chair of Fundamental and Applied Sciences Department (FASD)  
Universiti Teknologi PETRONAS

